portant in determining the frequency behavior of the eigenvalues of the periodic structure.

VII. Conclusions

We have presented wide-band equivalent circuits of closely resonant irises in rectangular waveguides. Poles and residues as functions of the geometry are provided so that the user need not refer to a computer program.

The above equivalent circuits constitute the building blocks of the network representation of an infinite waveguide periodically loaded with resonant irises, which we have investigated. The particular cases of capacitively and inductively periodically loaded waveguides are recovered from the general solution. The same network approach can be applied to waveguides loaded with other discontinuities.

References

[1] M. J. Al-Hakkak and Y. T. Lo, "Circular waveguides and horns with anisotropic and corrugated boundaries," Department of Electrical Engineering, Engineering Experiment Station, University of Illinois, Urbana, IL, Antenna Lab. Rep. No. 73-3, 1973.

[2] Y. T. Lo, "Feed investigation for large Thomson scatter radar," Dep. Elec. Eng., Univ. of Illinois, Urbana, IL, Aero. Rep. No. 23, Oct. 1967.

[3] R. Mittra and S. Lee, *Analytical Techniques in the Theory of Guided Waves*. New York, MacMillan, 1974.

[4] M. Navarro, "On waveguides with anisotropic and corrugated boundaries," Ph.D. dissertation, Elec. Eng. Dep. Univ. Illinois, Urbana, IL, 1976.

[5] J. Brown, "Propagation in coupled transmission line systems," *Quant. J. Mech. Appl. Math.*, vol. XI, pt. 2, pp. 235–243, 1958.

[6] T. E. Rozzi and W. F. G. Mecklenbrauker, "Wide-band network modeling of interacting inductive irises and steps," *IEEE Trans. Microwave Theory Tech.*, vol. MTT-23, pp. 235–245, Feb. 1975.

[7] T. E. Rozzi, "A new approach to the network modeling of capacitive irises and steps in waveguide," *Int. J. Circuit Theory Appl.*, vol. 3, pp. 339–354, Dec. 1975.

[8] T. Rozzi, "Network analysis of strongly coupled transverse apertures in waveguides," *Int. J. Circuit Theory Appl.*, vol. 1, pp. 161–178, June 1973.

[9] L. Lewin, *Advanced Theory of Waveguides*. London:Illiffe; 1952, p. 88.

[10] R. J. Mailloux: "Radiation and near field coupling between two co-linear open-ended waveguides," *IEEE Trans. Antennas Propagat.*, vol. AP-17, pp. 49–54, Jan. 1969.

[11] A. Jamieson and T. Rozzi, "Rigorous analysis of cross-polarization in flange-mounted rectangular waveguide radiators," Electron. Lett., vol. 13, no. 24, pp. 742–744, Nov. 1977.

[12] R. Collin, *Field Theory of Guided Waves*. New York:McGraw-Hill, 1962, p. 348.

Transmission Characteristics and a Design Method of Transmission-Line Low-Pass Filters with Multiple Pairs of Coincident Zeros and Multiple Pairs of Coincident Poles

JUNZI HURUYA AND RISABURO SATO, FELLOW, IEEE

Abstract—The transmission characteristics and a design method are presented for a transmission-line low-pass filter with multiple pairs of coincident zeros in the finite frequency of the passband and multiple pairs of coincident poles in the finite frequency of the stopband and for a transmission-line low-pass filter with Butterworth characteristic in the passband and multiple pairs of coincident poles in the finite frequency of the stopband. The former transmission-line low-pass filter shows an improved skirt attenuation performance and delay characteristic than a Chebyshev transmission-line low-pass filter in the same network degree. The latter type of transmission-line low-pass filter shows an improved skirt attenuation performance in comparison to a Butterworth transmission-line low-pass filter in the same network degree, it is positioned about in the middle between a Butterworth type and a Chebyshev type, the delay characteristic is improved considerably in comparison to the Chebyshev type, and the characteristic is close to that of the Butterworth type.

With this design method, the connecting unit elements in addition to the stubs contribute to the attenuation response. The design example is shown on the basis of a concrete specification, and it is shown that the obtained attenuation strictly fulfills the specification.

Manuscript received December 10, 1979; revised April 1, 1980.

J. Huruya is with the Department of Education, Yamaguchi University, Yamaguchi, Japan 753.

R. Sato is with the Department of Information Sciences, Tohoku University, Sendai, Japan 980.

I. Introduction

RECENTLY, Levy [1] has shown a lumped element rational function having single transmission zeros in one point of the stopband of a Chebyshev low-pass filter which shows improvement of the skirt selectivity over an ordinary Chebyshev low-pass filter. By use of cross coupling, the realization of a high frequency filter is executed. Further, M. C. Agarwal [2] has proposed a lumped element rational function having multiple pairs of coincident

0018-9480/80/0800-0865$00.75

poles in one point of the stopband for a Chebyshev low-pass filter.

In this paper, a transmission-line low-pass filter having multiple pairs of coincident zeros in a finite frequency of the passband (in addition to the zeros at the origin) and multiple pairs of coincident poles in a finite frequency of the stopband (including single pairs of poles), which in regard to the attenuation characteristic shows a different passband from filters shown in the literature [1] and [2], but a similar stopband, is treated, and its transmission characteristic and a design method are described. Further, as a filter resembling those shown in the literature [3] and [4], a transmission-line low-pass filter having the Butterworth characteristic in the passband and having multiple pairs of coincident poles in the finite frequency of the stopband is treated. For the treated transmission-line low-pass filters, the contribution of connecting unit elements to the attenuation response in addition to stubs is taken into consideration.

The conformal mapping is used for the complex frequency plane of the characteristic function of a lumped element Butterworth low-pass filter and the complex frequency plane of the characteristic function of the above transmission-line low-pass filter is derived, and when the maximum attenuation in the pass-band and the minimum attenuation in the stopband are given as specifications, design equations under consideration of strict fulfillment of this specification are derived.

The former transmission-line low-pass filter has an improved cutoff characteristic than a Chebyshev transmission-line low-pass filter [5] for the same network degree, it is positioned about in the middle between a Chebyshev type and an elliptic-function type [6]–[8], and the delay characteristic is improved over these two type of filters. The frequency of poles and that of zeros are decided by the assignation of a network degree, a number of connecting unit elements, an order of poles and zeros, a passband cutoff frequency, a maximum attenuation in the passband and a minimum attenuation in the stopband, but inversely frequencies of poles and zeros can be assigned arbitrarily. The application in case of assigning poles and zeros can be exemplified for a multiharmonic rejection filter [12]. It does appear that this type of the filter can be adoptable as that having a different transmission characteristic from ordinary filters.

A design example for the transmission-line low-pass filter is shown on the basis of concrete specifications. Also, it is shown that this type of the filter treated in this paper has a smaller spread of elements than the elliptic-function type filter for the same bandwidth.

The latter transmission-line low-pass filter has an improved cutoff characteristic than a Butterworth transmission-line low-pass filter for the same network degree, it is positioned about in the middle between the Butterworth type and the Chebyshev type, the delay characteristic is improved considerably over the Chebyshev type for the entire passband, and it resembles and approaches the delay characteristic of the Butterworth type.

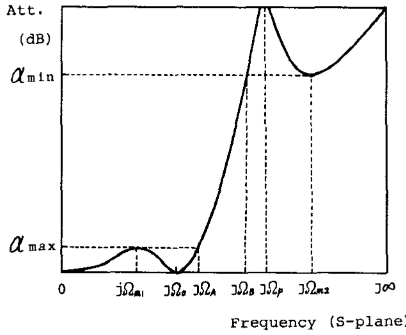

Fig. 1. Attenuation response of the transmission-line low-pass filter with zeros of m'th order at $\pm j\Omega_0$ and poles of mth order at $\pm j\Omega_p$.

II. Transmission Line Filter With Multiple Pairs of Coincident Zeros in the Passband and Multiple Pairs of Coincident Poles in the Stopband

A. Derivation of Design Equations (Transformed Equations)

When the lengths of the lossless transmission-line all are 1/4 of the wavelength corresponding to the standard frequency f_0, Richards transformation [9] becomes as follows:

$$S = j\tan(\pi f/2f_0) \tag{1}$$

so that the actual frequency range (f-plane) is transformed to the S-plane. When r connecting unit elements contribute to the attenuation response, the characteristic function of the transmission-line filter has poles of $(r/2)$th order at $S=\pm 1.0$. Therefore, as shown in Fig. 1, when a transmission-line low-pass filter with the attenuation characteristic in the S-plane has zeros of m'th order at $\pm j\Omega_0$ in the passband, zeros of lth order at the origin, poles of mth order at $\pm j\Omega_p$ in the stopband, and poles of qth order at the infinite point, the relation between the network degree n and the number of connecting unit elements r is given by

$$n = 2m + q + r = 2m' + l, \qquad r = 2p. \tag{2}$$

It is necessary to consider the (2) in order to derive the treated transmission-line low-pass filter from the lumped element Butterworth low-pass filter by using the conformal mapping.

When for a lumped element Butterworth low-pass filter with a network degree of nth degree the maximum attenuation in the passband α_{max}(dB) and the minimum attenuation in the stopband α_{min}(dB) are given specifications, with the passband cutoff frequency $j1.0$ and the stopband cutoff frequency jk_1, and the frequency jt_x is assumed to provide an arbitrary attenuation α_x(dB), then the following relation [10] holds:

$$k_1 = \left[(10^{0.1\alpha_{min}} - 1)/(10^{0.1\alpha_{max}} - 1)\right]^{1/2n} \tag{3}$$

$$t_x = \left[(10^{0.1\alpha_x} - 1)/(10^{0.1\alpha_{max}} - 1)\right]^{1/2n}. \tag{4}$$

When the complex frequency plane of this lumped element Butterworth low-pass filter is taken as the t-plane,

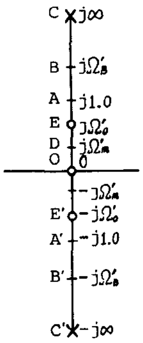

Fig. 2. ξ-plane. O zeros. × poles.

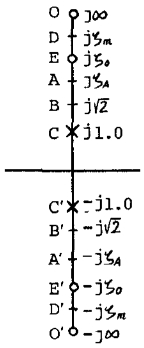

Fig. 3. ζ-plane. O zeros. × poles.

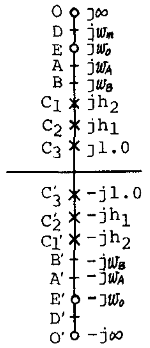

Fig. 4. W-plane. O zeros. × poles.

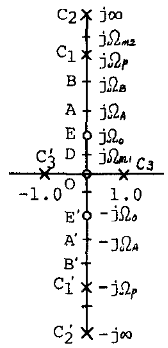

Fig. 5. S-plane. O zeros. × poles.

TABLE I
CORRESPONDING RELATION AMONG EACH PLANE

Plane	O	D	E	A	B	C		
ξ-plane	0.0	$\pm j\Omega'_m$	$\pm j\Omega_0$	$\pm j1.0$	$\pm j\Omega'_B$	$\pm j\infty$		
ζ-plane	$\pm j\infty$	$\pm j\zeta_m$	$\pm j\zeta_0$	$\pm j\zeta_A$	$\pm j\sqrt{2}$	$\pm j1.0$		
W-plane	$\pm j\infty$	$\pm jW_m$	$\pm jW_0$	$\pm jW_A$	$\pm jW_B$	$\pm j1.0$	$\pm jh_1$	$\pm jh_2$
S-plane	0.0	$\pm j\Omega_{m1}$	$\pm j\Omega_0$	$\pm j\Omega_A$	$\pm j\Omega_B$	± 1.0	$\pm j\infty$	$\pm j\Omega_p$

the transformed equations from the t-plane to the complex frequency of a lumped element low-pass filter with zeros of m'th order in the passband (ξ-plane in Fig. 2) become as follows [11]:

$$\xi^{n-2m'}(\xi^2+\Omega_0'^2)^{m'}=(1-\Omega_0'^2)^{m'}t^n \tag{5}$$

$$C_0\Omega_0'^n=(1-\Omega_0'^2)^{m'} \tag{6}$$

$$C_0^2=(n-2m')^{n-2m'}(2m')^{2m'}/n^n \tag{7}$$

$$\Omega_m'^2=(n-2m')\Omega_0'^2/n \tag{8}$$

where $\xi=\Sigma'+j\Omega'$ applies. Ω'_0 is zeros of m'th order in the ξ-plane, Ω'_m is the frequency providing the maximum attenuation (peak value) in the passband of the ξ-plane. The passband cutoff frequency is normalized to $j1.0$.

When the transformation to the ζ-plane shown in Fig. 3 is executed on the ξ-plane for the corresponding relation of Table I, the transformed equation becomes

$$\zeta^2=\Omega_B'^2/\xi^2-1. \tag{9}$$

Ω'_B is the stopband cutoff frequency in the ξ-plane. Next, the separation transformation is executed so that poles of $n/2$th order at $\pm j1.0$ in the ζ-plane become poles of pth, $(n/2-p-m)$th, and mth order at $\pm j1.0$, $\pm jh_1$, $\pm jh_2$, respectively, in the W-plane shown in Fig. 4, for which the transformed equation is given by (10). (For the derivation of (10), refer to the Appendix.)

$$(W^2+1)^p(W^2+h_1^2)^{n/2-p-m}(W^2+h_2^2)^m(W^2+w_0^2)^{-m'}=(\zeta^2+1)^{n/2}(\zeta^2+\zeta_0^2)^{-m'}. \tag{10}$$

Finally, the transformation to the S-plane shown in Fig. 5 is executed with (11) for the corresponding relation of Table I

$$S^2=(h_1^2-1)/(W^2+h_1^2), \qquad S=\Sigma+j\Omega. \tag{11}$$

Poles at $S=\pm 1.0$ have pth order, poles at $\pm j\Omega_p$ have mth order, poles at the infinite point have $q(=n-2m-2p)$th order, zeros at $\pm j\Omega_0$ have m'th order, and zeros at the origin have $l(=n-2m')$th order.The S-plane is thus the complex frequency plane for the characteristic function of the transmission-line low-pass filter to be obtained, and the (2) is established.

By use of the corresponding relation in Table I and (9) to (11), the direct transformed (12) from the ξ-plane to the S-plane can be derived

$$(h_1^2-1)^{n/2-m'}(S^{-2}-1)^p(S^{-2})^{n/2-p-m}\cdot(S^{-2}+\Omega_p^{-2})^m(S^{-2}+\Omega_0^{-2})^{-m'}=\Omega_B'^{n-2m'}\Omega_0'^{2m'}/\left[\xi^{n-2m'}(\xi^2+\Omega_0'^2)^{m'}\right]. \tag{12}$$

As the passband cutoff frequency $j1.0$ in the ξ-plane corresponds to the passband cutoff frequency $j\Omega_A$ in the S-plane, h_1 is obtained from (12). When the obtained h_1 is substituted into (12)

$$S^{2m'-n}(1-S^2)^p(1+\Omega_p^{-2}S^2)^m(1+\Omega_0^{-2}S^2)^{-m'} = \frac{(1-\Omega_0'^2)^{m'}\Omega_A^{2m'-n}(1+\Omega_A^2)^p \cdot(1-\Omega_A^2\Omega_p^{-2})^m(\Omega_A^2\Omega_0^{-2}-1)^{-m'}}{\xi^{n-2m'}(\xi^2+\Omega_0'^2)^{m'}} \tag{13}$$

is obtained, and by use of (5)

$$S^{2m'-n}(1-S^2)^p(1+\Omega_p^{-2}S^2)^m(1+\Omega_0^{-2}S^2)^{-m'} = \Omega_A^{2m'-n}(1+\Omega_A^2)^p(1-\Omega_A^2\Omega_p^{-2})^m(\Omega_A^2\Omega_0^{-2}-1)^{-m'}t^{-n} \tag{14}$$

is obtained. The (14) is the direct transformation from the t-plane to the S-plane.

When here the passband cutoff frequency f_A in the actual frequency range (f-plane) corresponding to the passband cutoff frequency Ω_A in the S-plane or the bandwidth W (%) (in regard to f_0) in case of regarding lowpass filters as bandstop filters, is given

$$\Omega_A = \tan\frac{\pi f_A}{2f_0} = \tan\frac{\pi}{2}\left(1-\frac{W}{200}\right) \tag{15}$$

is obtained from (1).

As the frequency $j\Omega_m'$ providing the maximum attenuation in the passband of the ξ-plane corresponds to the frequency $j\Omega_{m1}$ providing the maximum attenuation in the passband of the S-plane, the (16) is obtained from (13) by use of (6) to (8)

$$\Omega_0^2 = (\Omega_{m1}^2+\sigma_1\Omega_A^2)/(\sigma_1+1) \tag{16}$$

where

$$\sigma_1 = \left(\frac{\Omega_A}{\Omega_{m1}}\right)^{(n-2m')/m'}\left(\frac{\Omega_{m1}^2+1}{\Omega_A^2+1}\right)^{p/m'}\left[\frac{\Omega_p^2-\Omega_{m1}^2}{\Omega_p^2-\Omega_A^2}\right]^{m/m'}. \tag{17}$$

The characteristic function $K(S)$ in the S-plane is expressed as

$$K(S) = \frac{C_K S^{n-2m'}(S^2+\Omega_0^2)^{m'}}{(1-S^2)^p(S^2+\Omega_p^2)^m} \tag{18}$$

where C_K is a real constant. Moreover, the operating attenuation function $L(j\Omega)$ is expressed as

$$L(j\Omega) = 10\log[1+|K(j\Omega)|^2]. \tag{19}$$

By differentiation of (19) with Ω, the frequency Ω_{m1} providing the maximum attenuation in the passband and the frequency Ω_{m2} providing the minimum attenuation in the stopband can be obtained, and they are the positive solutions of the following three degree equation in regard to Ω^2

$$q(\Omega^2)^3 + [n-2m+(2p-n)\Omega_p^2+(2m'-q)\Omega_0^2](\Omega^2)^2 + [(2m+2m'-n)\Omega_0^2 - n\Omega_p^2 + (n-2m'-2p)\Omega_p^2\Omega_0^2]\Omega^2 + (n-2m')\Omega_p^2\Omega_0^2 = 0 \tag{20}$$

with $q = n-2m-2p$. Equation (20) has two positive solutions and one negative solution in regard to Ω^2. The smaller of the positive solution is taken as Ω_{m1}^2, and the larger one as Ω_{m2}^2. Further, as the attenuation $L(j\Omega_A)$ occurring at the passband cutoff frequency $j\Omega_A$ must become $\alpha_{\max}$(dB) of the specification and the minimum attenuation $L(j\Omega_{m2})$ in the stopband must fulfill $\alpha_{\min}$(dB) of the specification

$$|K(j\Omega_A)|^2 = 10^{0.1\alpha_{\max}}-1 \qquad |K(j\Omega_{m2})|^2 = 10^{0.1\alpha_{\min}}-1 \tag{21}$$

are established. By use of (3), the relation between Ω_p and Ω_{m2} is derived as

$$\Omega_p^2 = (\sigma_2\Omega_{m2}^2+\Omega_A^2)/(\sigma_2+1) \tag{22}$$

from (21), where

$$\sigma_2 = k_1^{n/m}\left(\frac{\Omega_A}{\Omega_{m2}}\right)^{(n-2m')/m}\left(\frac{\Omega_{m2}^2+1}{\Omega_A^2+1}\right)^{p/m}\left(\frac{\Omega_A^2-\Omega_0^2}{\Omega_{m2}^2-\Omega_0^2}\right)^{m'/m}. \tag{23}$$

Accordingly, when $\alpha_{\max}, \alpha_{\min}$, and Ω_A are specified and m, p, and m' are given, Ω_{m1}, Ω_{m2}, Ω_0, and Ω_p can be obtained from (16), (20), and (22). By use of the obtained Ω_p and Ω_0, the stopband cutoff frequency and the frequency providing the arbitrary attenuation (the frequency in the range $\Omega_0<\Omega<\Omega_p$) in the S-plane can be obtained from the t-plane (by use of values obtained by (3) and (4)) by means of (14). In this case, the attenuation at Ω_{m1} and Ω_{m2} sufficiently fulfills the specification.

B. Relation Between the Specification and the Skirt Attenuation

Since the stopband cutoff frequency jk_1 in the t-plane corresponds to the stopband cutoff frequency $j\Omega_B$ in the S-plane, Ω_B is obtained from (14) as follows:

$$\Omega_B^{2m'-n}(\Omega_B^2+1)^p(1-\Omega_B^2\Omega_p^{-2})^m = K_{01}k_1^{-n}(\Omega_B^2\Omega_0^{-2}-1)^{m'} \tag{24}$$

where

$$K_{01} = \Omega_A^{2m'-n}(\Omega_A^2+1)^p(1-\Omega_A^2\Omega_p^{-2})^m(\Omega_A^2\Omega_0^{-2}-1)^{-m'}. \tag{25}$$

As k_1^n is decided by $\alpha_{\max}$ and $\alpha_{\min}$ of the specification as shown in (3), the (24) shows the relation between the specification and the network degree n, the number of connecting unit elements $r(=2p)$, and the stopband cutoff frequency Ω_B (the skirt selectivity). Now occurs the problem of how to decide the order m' of the zero point Ω_0 in the passband. For this, it is sufficient to obtain the m' which provides a minimum Ω_B when n is held constant in (24). In regard to the various values of n, the consolidation of the results of actual calculations shows that the best skirt selectivity is obtained when m' is decided as follows:

$$\begin{aligned} m' &= (n-1)/4, && \text{for } n = 4n'+1\\ m' &= (n-2)/4, && \text{for } n = 4n'+2\\ m' &= (n+1)/4, && \text{for } n = 4n'+3\\ m' &= n/4, && \text{for } n = 4n'+4, \quad n' = 1,2,3,\ldots. \end{aligned} \tag{26}$$

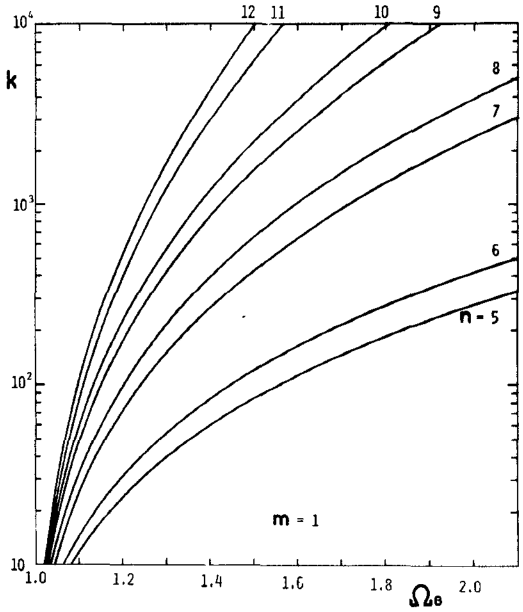

Fig. 6. Relation between k and Ω_B.

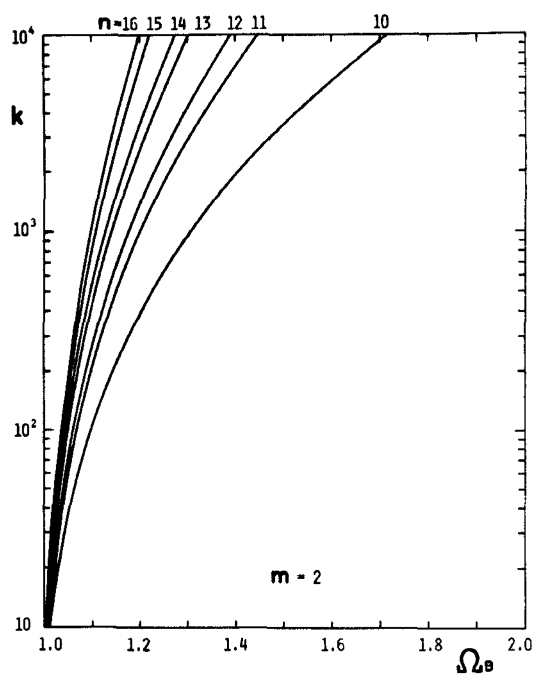

Fig. 7. Relation between k and Ω_B.

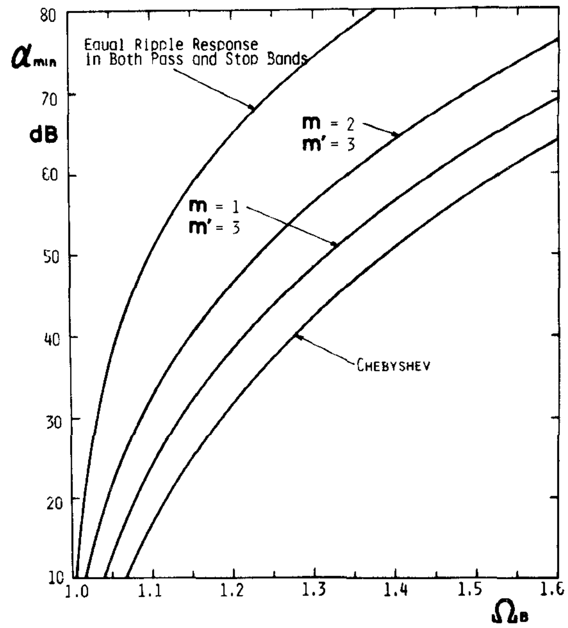

Fig. 8. Comparison of skirt attenuation performance ($n=12$).

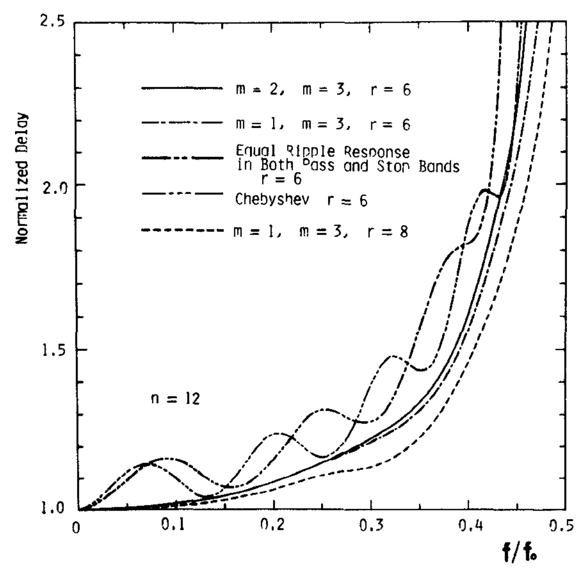

Fig. 9. Comparison of delay characteristics ($n=12$).

When here the number of connecting unit elements $r(=2p)=n/2$ is taken for an even n, $r=(n-1)/2$ for an odd n, and Ω_A is 1 $(f_A=0.5f_0), k(=k_1^n)$ specified by the specification and the stopband cutoff frequency Ω_B is shown by Figs. 6 and 7 in the graphic form for $n=5$ to 16. The order m' of Ω_0 is decided according to (26), and when the order m of Ω_p is 1 or 2, Ω_B is calculated from (16), (20), (22), and (24). The network synthesis is possible by deciding the characteristic function $K(S)$, obtaining the operating transfer factor $S_B(S)$ from the relation $|S_B(S)|^2 = 1+|K(S)|^2$, and obtaining the driving-point impedance $Z_{11}(S)$ or the admittance $Y_{11}(S)$ from $K(S)$ and $S_B(S)$.

C. Comparison of the Skirt Selectivity and Comparison of the Delay Characteristic

The skirt selectivity of the transmission-line low-pass filter treated in this chapter and that of the Chebyshev transmission-line low-pass filter [5] and that of the transmission-line filter having equal ripple response in both passbands and stopbands (elliptic-function type) [6] are compared. When the network degree n is 12th degree, the number of connecting unit elements r is 6, the maximum attenuation α_{max} in the passband is 0.1(dB), and the passband cutoff frequency Ω_A is 1, in each filter, the relation in the S-plane between the stopband cutoff frequency Ω_B and the minimum attenuation α_{min}(dB) in the stopband for each low-pass filter can be shown graphically as shown in Fig. 8. The skirt selectivity for the filter treated in this chapter is inferior to the elliptic-function type for $m=2$ as well as $m=1$, but it is improved over the Chebyshev type, and it is positioned about in the middle between these two types.

Next, the delay characteristics are compared. For $n=12$, $r=6$, $\Omega_A=1$, $\alpha_{\max}=0.5$(dB), and $\alpha_{\min}=40.0$(dB), the delay characteristics for the actual frequency range (f-plane) of each filter are shown in Fig. 9. The delay at each frequency is normalized by the delay occurring at $f=0$ ($\Omega=0$). For $m=2$ as well as $m=1$, the delay characteristics have the smooth response and are improved over the Chebyshev type and the elliptic-function type. Furthermore, Fig. 9 also shows the delay characteristic for $n=12$, $m=1$, $m'=3$, and $r=8$ (the number of connecting unit elements is increased by 2 while the other conditions are unchanged), and it can be seen that the delay characteristic is improved over the case of $r=6$, and that the contribution of connecting unit element to the delay characteristic is larger than that of stubs.

III. Transmission-Line Low-Pass Filter With Multiple Pairs of Coincident Poles in the Stopband

A. Derivation of Design Equations (Transformed Equations)

A transmission-line low-pass filter as shown in Fig. 10 with Butterworth characteristic in the passband, poles of mth order at $\pm j\Omega_p$ in the stopband, and poles of lth order at the infinite point is treated. At this time

$$n=2m+l+r, \qquad r=2p \tag{27}$$

is established between the network degree n and the number of connecting unit elements r. The transformed equation from the t-plane (the plane of a lumped element Butterworth low-pass filter) shown in Fig. 11 to the λ-plane shown in Fig. 12 is expressed as

$$\lambda^2=k_1^2/t^2-1. \tag{28}$$

Next, the separation transformation is executed so that poles of $n/2$th order at $\pm j1.0$ in the λ-plane become poles of pth, $(n/2-p-m)$th, and mth order at $\pm j1.0$, $\pm jh_1$, $\pm jh_2$, respectively, in the η-plane shown in Fig. 13. The transformed equation is as follows:

$$(\eta^2+1)^p(\eta^2+h_1^2)^{n/2-p-m}(\eta^2+h_2^2)^m=(\lambda^2+1)^{n/2}. \tag{29}$$

Further, the η-plane is transformed to the S-plane shown in Fig. 14 by (30)

$$S^2=(h_1^2-1)/(\eta^2+h_1^2), \qquad S=\Sigma+j\Omega. \tag{30}$$

The S-plane is the complex frequency plane for the characteristic function of the transmission-line low-pass filter to be obtained. By use of (28)–(30) and of the relation that the passband cutoff frequency $j1.0$ in the t-plane corresponds to $j\Omega_A$ in the S-plane, the direct transformed equation from the t-plane to the S-plane is derived as follows:

$$(S^{-2})^{n/2-p-m}(S^{-2}-1)^p(S^{-2}+\Omega_p^{-2})^m$$
$$=j^{2n}\Omega_A^{-n}(\Omega_A^2+1)^p(1-\Omega_p^{-2}\Omega_A^2)^m\, t^{-n}. \tag{31}$$

In this case, the characteristic function $K(S)$ in the S-

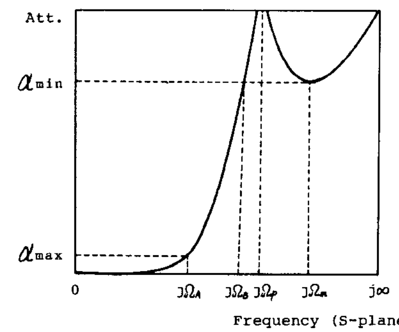

Fig. 10. Attenuation response of the transmission-line low-pass filter with poles of mth order at $\pm j\Omega_p$ in the stopband.

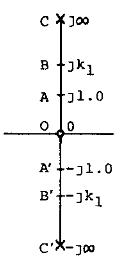

Fig. 11. t-plane. ○ zeros. × poles.

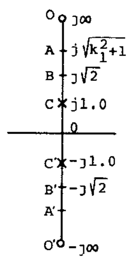

Fig. 12 λ-plane. ○ zeros. × poles.

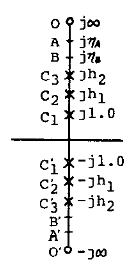

Fig. 13. η-plane. ○ zeros. × poles.

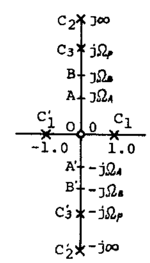

Fig. 14. S-plane. ○ zeros. × poles.

plane is expressed as

$$K(S)=C_K S^n/\left[(1-S^2)^p(S^2+\Omega_p^2)^m\right] \tag{32}$$

where C_K is a real constant. As the operating attenuation function $L(\Omega)$ is expressed by (19), the frequency Ω_m providing the minimum attenuation in the stopband is obtained by $dL(j\Omega)/d\Omega=0$, which is the positive solution fulfilling the following equation:

$$(n-2m-2p)\cdot\Omega_m^4+\left[(2p-m)\cdot\Omega_p^2+n-2m\right]\cdot\Omega_m^2-n\cdot\Omega_p^2=0. \tag{33}$$

Also, from $|K(j\Omega_A)|^2=10^{0.1\alpha_{\max}}-1$ and $|K(j\Omega_m)|^2=10^{0.1\alpha_{\min}}-1$, the relation between Ω_p and Ω_m, Ω_A is derived as follows:

$$\Omega_p^2=\frac{k_1^{n/m}\Omega_A^{n/m}\Omega_m^2(\Omega_m^2+1)^{p/m}+\Omega_A^2(\Omega_A^2+1)^{p/m}\Omega_m^{n/m}}{k_1^{n/m}\Omega_A^{n/m}(\Omega_m^2+1)^{p/m}+(\Omega_A^2+1)^{p/m}\Omega_m^{n/m}}. \tag{34}$$

When (34) is substituted into (33) and Ω_p is eliminated

$$\begin{aligned}&(\Omega_A^2+1)^{p/m}\cdot\Omega_m^{n/m-2}\left[(n-2m-2p)\cdot\Omega_m^4+((2p-n)\right.\\&\left.\cdot\Omega_A^2+n-2m)\cdot\Omega_m^2-n\cdot\Omega_A^2\right]\\&-2mk_1^{n/m}\cdot\Omega_A^{n/m}(\Omega_m^2+1)^{p/m+1}=0\end{aligned} \tag{35}$$

is obtained. When $\alpha_{\min}$, $\alpha_{\max}$, and Ω_A are given as the specification, Ω_m fulfilling the specification can be obtained from (35), as k_1 is decided by (3), and the poles Ω_p can be obtained from (34). By use of the obtained Ω_p and (31), the stopband cutoff frequency Ω_B in the S-plane and the frequency providing the arbitrary attenuation (the frequency in the range $0<\Omega<\Omega_p$) can be obtained from the t-plane.

B. Comparison of the Skirt Selectivity and Comparison of the Delay Characteristic

The skirt selectivity of a transmission-line low-pass filter with poles of mth order in the stopband, of a Chebyshev transmission-line low-pass filter, and of a Butterworth transmission-line low-pass filter is compared in the S-plane. $n=12$, $r=6$, $\Omega_A=1$, and $\alpha_{\max}=0.5$(dB) are used for each filter, and the relation between the stopband cutoff frequency Ω_B and the minimum attenuation $\alpha_{\min}$(dB) in the stopband is shown in Fig. 15. The skirt selectivity for the filter treated in this chapter is inferior to the Chebyshev type for $m=2$ as well as $m=1$, but it is superior to the Butterworth type, and it is positioned about in the middle between these two types. Next, the comparison of the delay characteristic in the f-plane for $n=12$, $r=6$, $\Omega_A=1$, $\alpha_{\max}=0.5$(dB), and $\alpha_{\min}=40.0$(dB) is shown in Fig. 16. The delay occurring at each frequency is normalized by the delay occurring at $f=0$. The delay characteristic of the filter having poles of $m=1$ or $m=2$ in the stopband is more improved than the delay characteristic of the Chebyshev filter, and resembles and approaches the delay characteristic of the Butterworth filter. Also, Figs. 15 and 16 show the skirt selectivity and the delay characteristic for $m=1$ and $r=8$. (The other conditions are the same.) The delay characteristic at this time is superior to that of the Butterworth type for $r=6$, and the cutoff characteristic also is superior to the Butterworth type.

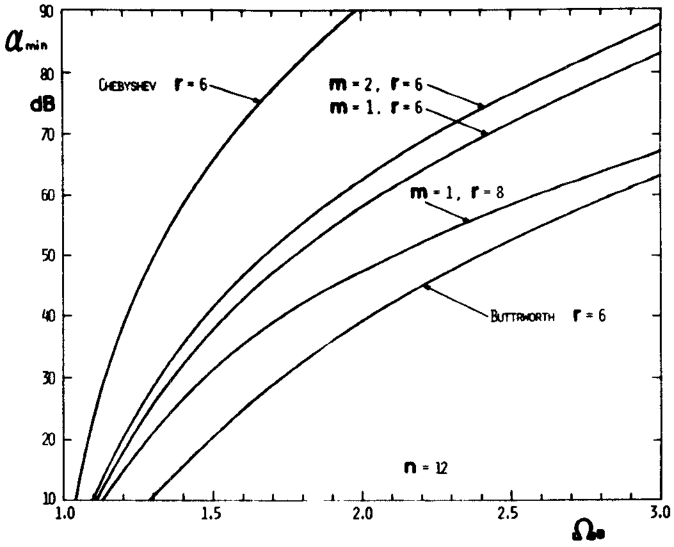

Fig. 15. Comparison of skirt attenuation performance ($n=12$).

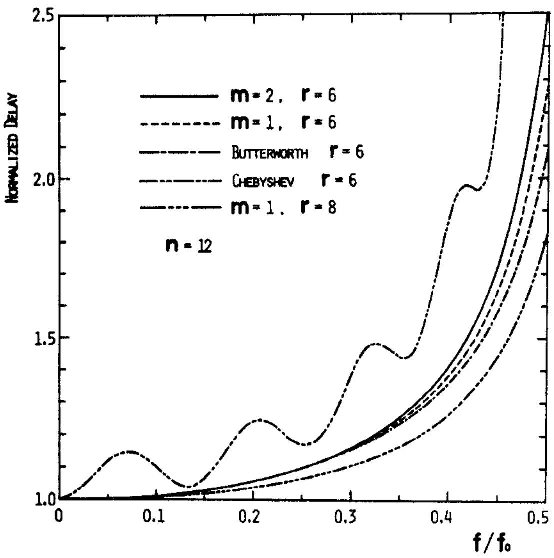

Fig. 16. Comparison of delay characteristics ($n=12$).

IV. Design Example

A. Design Example for a Transmission-Line Low-Pass Filter Having Poles of mth Order and Zeros of m′th Order

The transmission-line low-pass filter is designed on the basis of the following specification:

maximum attenuation in the passband	$\alpha_{\max}=0.1$(dB)
minimum attenuation in the stopband	$\alpha_{\min}=30.0$(dB)
passband cutoff frequency	$f_A=0.5f_0$
network degree	$n=12$.

As $n=12$ is used, $q=2$ and $l=6$ are obtained from (2) for $r=6$, $m=2$, and $m'=3$ (by (26)). From (15), the

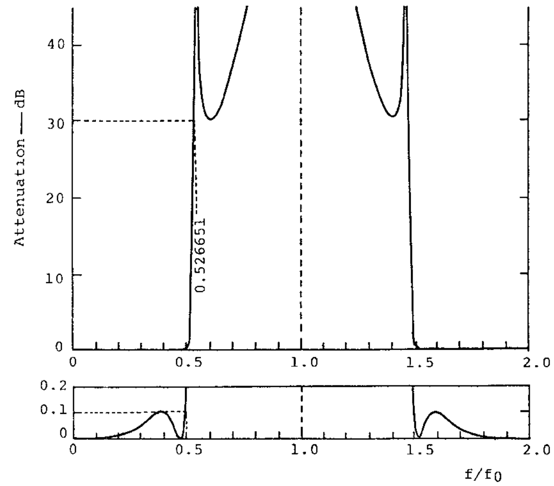

Fig. 17. Attenuation response of a transmission-line low-pass filter ($n=12$, $m=2$, $m'=3$, $r=6$).

TABLE II
CALCULATING RESULTS OF THE EXAMPLE

Ω	Calculated values	Attenuation (dB)	Ω	Calculated values	Attenuation (dB)
Ω_{m1}	0.6711611	0.1000000	Ω_B	1.0874383	30.0000000
Ω_0	0.9357692	0.0	Ω_{40}	1.1001630	40.0000000
Ω_A	1.0000000	0.1000000	Ω_{50}	1.1090934	50.0000000
Ω_{10}	1 0507095	10.0000000	Ω_p	1.1234816	∞
Ω_{20}	1.0708674	20.0000000	Ω_{m2}	1.3274583	30.0000000

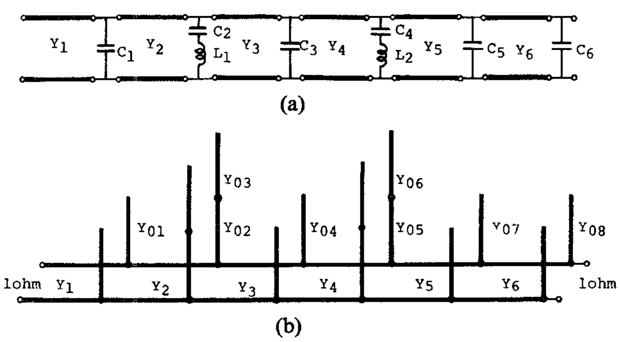

Y_1=0.902630 Y_2=0.797555 Y_3=0.528402 Y_4=0.578046
Y_5=0.659894 Y_6=0.532684 Y_{01}=0.670030 Y_{02}=0.266256
Y_{03}=0.210944 Y_{04}=1.608298 Y_{05}=0.378366 Y_{06}=0.299764
Y_{07}=1.368792 Y_{08}=0.575189

Fig. 18. Realized network.

passband cutoff frequency in the S-plane becomes $\Omega_A=1$. When Ω_{m1}, Ω_{m2}, Ω_p, and Ω_0 are obtained from (16), (20), and (22), and when the stopband cutoff frequency Ω_B is obtained from (24), the values shown in Table II are obtained. Further, when the frequencies t_{10}, t_{20}, t_{40}, and t_{50} providing 10, 20, 40, 50 (dB) in the t-plane are obtained from (4), and their corresponding frequencies Ω_{10}, Ω_{20}, Ω_{40}, and Ω_{50} in the S-plane are obtained from (14), the values shown in Table II are obtained. The Newton–Raphson method is used for the calculation for (20), (24), and (14), and 1×10^{-10} is used as the convergence judgment value. The calculated values of the attenuation occurring at each obtained frequency are shown in the right column of Table II. When the frequenicies were obtained to the 11th decimal, the difference between the calculated attenuation at each frequency and the specification or the designated attenuation were within 1×10^{-9}, and values sufficiently fulfilling the specification or the designated attenuation could be obtained from the design equation.

The attenuation characteristic at the actual frequency range (f-plane) is shown in Fig. 17, and the low-pass filter is obtained in the frequency range from 0 to f_0, while the bandstop filter is obtained in the range 0 to $2f_0$.

For this case, the network synthesis is to be obtained. The characteristic function $K(S)$ is expressed by

$$K(S)=\frac{C_K S^6(S^2+0.9357692^2)^3}{(1-S^2)^3(S^2+1.1234816^2)^2} \tag{36}$$

$C_K=43.6731502$ is obtained from $L(j\Omega_A)=0.1$(dB). From the relation $|S_B(S)|^2=1+|K(S)|^2$, the operating transfer factor $S_B(S)$ is obtained as follows:

$$\begin{aligned}S_B(S)=43.6731502(&S^{12}+3.4771142S^{11}+8.6721537S^{10}\\&+15.3237456S^9+21.4304570S^8+24.1073068S^7\\&+22.0984645S^6+16.4794984S^5+9.8500294S^4\\&+4.5722531S^3+1.5521017S^2+0.3420632S\\&+0.0364795)/\left[(1-S^2)^3(S^2+1.1234816^2)^2\right].\end{aligned} \tag{37}$$

From $S_B(S)$ and $K(S)$, the driving-point impedance $Z_{11}(S)$ is obtained as follows:

$$\begin{aligned}Z_{11}(S)&=\frac{S_B(S)+S_B(-S)+K(S)+K(-S)}{S_B(S)-S_B(-S)-K(S)+K(-S)}\\&=(2.0S^{12}+11.2991459S^{10}+23.7308198S^8+22.7699129S^6\\&\quad+9.8500294S^4+1.5521017S^2+0.0364795)\\&\quad/(3.4771142S^{11}+15.3237456S^9+24.1073068S^7\\&\quad+16.4794984S^5+4.5722531S^3+0.3420632S).\end{aligned} \tag{38}$$

When attention is paid to attenuation poles and the number of connecting unit elements and the removal of elements is executed from $Z_{11}(S)$, the network shown in Fig. 18(a) is obtained, and it is changed further to Fig. 18(b). Each element value is the characteristic admittance, the values for the internal resistance of the power source and the load resistance both being 1 Ω.

B. Comparison of the Element Value

For $n=12$, $r=6$, $\alpha_{max}=0.1$(dB), and $\alpha_{min}=30.0$(dB), when the transmission-line low-pass filter is considered as the transmission-line bandstop filter, the comparison of the spread of element values (characteristic admittances) accompanying the change of the bandwidth W (%) is executed for the filter treated in Section II and the elliptic-function type filter. Table III shows characteristic admittances of each element in the network shown in Fig. 18(b) and the ratio of the maximum element value to the minimum element value in case of the filter with $m=2$ and $m'=3$. Table IV shows the ratio of the maximum element value to the minimum element value for the elliptic-function type filter [6] which is synthesized with the same network as shown in Fig. 18(b). As the bandwidth becomes broad, it can be seen that the filter treated in this paper has a smaller spread of element values than the elliptic-function type filter for the same bandwidth.

TABLE III
RELATION BETWEEN THE BANDWIDTH W OF THE TRANSMISSION-LINE BANDSTOP FILTER AND VALUES OF ELEMENTS
($n=12$, $m=2$, $m'=3$, $r=6$, $\alpha_{max}=0.1$(dB), $\alpha_{min}=30.0$(dB))

W(%)	Y_1 Y_{02}	Y_2 Y_{03}	Y_3 Y_{04}	Y_4 Y_{05}	Y_5 Y_{06}	Y_6 Y_{07}	Y_{01} Y_{08}	Max, value / Min. value
50(%)	0.976845 0.229700	0.946082 0.025758	0.742720 0.563521	0.811922 0.337900	0.840092 0.037888	0.746639 0.475829	0,158812 0.268462	37.92
100(%)	0.902630 0.266256	0.797555 0.210944	0.528402 1.608298	0.578046 0.378366	0.659894 0.299764	0.532684 1.368792	0.670030 0.575189	7.62
110(%)	0.871513 0.253591	0.745986 0.281495	0.481975 1.939217	0.526933 0.357494	0.611655 0.396831	0.485812 1.658250	0.881456 0,661617	7.65
120(%)	0.831220 0.236313	0.685845 0,368987	0.433904 2.342427	0.473978 0.330528	0.558497 0.516097	0.437558 2.013497	1.157150 0,765494	9.91
130(%)	0.779607 0.215082	0.617599 0.478900	0.384154 2.846455	0.419224 0.298606	0.500535 0.664876	0.387761 2.459903	1,519487 0.894934	13.23

TABLE IV
RELATION BETWEEN THE BANDWIDTH W OF THE ELLIPTIC-FUNCTION TYPE TRANSMISSION-LINE FILTER AND VALUES OF THE ELEMENTS
($n=12$, $r=6$, $\alpha_{max}=0.1$(dB), $\alpha_{min}=30$(dB))

W(%)	Y_1 Y_{02}	Y_2 Y_{03}	Y_3 Y_{04}	Y_4 Y_{05}	Y_5 Y_{06}	Y_6 Y_{07}	Y_{01} Y_{08}	Max. value / Min. value
50(%)	0.748243 0.112899	0.805047 0.017330	0.706962 0.468131	0.675143 0.281515	0.690669 0.035208	0.616250 0.527822	0.249485 0.369776	46.45
100(%)	0.568883 0.098258	0.657406 0.093875	0.523477 1.377211	0.504261 0.245869	0.532452 0.218743	0.400710 1.405940	0.995710 0.894712	14.98
110(%)	0.523574 0.089245	0.610950 0.117601	0.479573 1.673548	0.463528 0.223287	0.491597 0.277115	0.359447 1.684880	1.257359 1.044458	18.88
120(%)	0.475096 0.079437	0.559037 0.145357	0.433206 2.036068	0.420123 0.192020	0.454336 0.333861	0.318613 2.006271	1.580410 1.254467	25.63
130(%)	0.423507 0.069227	0.499941 0.178748	0.386077 2.507586	0.350372 0.035441	0.608907 0.087555	0.258802 2.276928	1.989436 1.913264	70.75

Here, when α_{max} and α_{min} are given as specifications, the method of [6] requires more computing time than our design method in order to obtain zeros and poles. Also, in the method of [6], the attenuation at an obtained stopband cutoff frequency fulfills α_{min} of the specification, but when frequencies Ω_{M1}, $\Omega_{M2}(\Omega_{M2}>\Omega_{M1})$ providing the minimum attenuation in the stopband are obtained, the attenuation at this Ω_{M2} does not fulfill α_{min}(dB) and it shows a tendency to deviate from α_{min}. For instance, when $\alpha_{min}=30.0$(dB) is given as the specification, the attenuation at Ω_{M2} for W = 120% is 26.5313(dB) and the attenuation at Ω_{M2} for W = 130% is 25.7777(dB). In our design method, the minimum attenuation in the stop band strictly fulfills α_{min}(dB).

V. CONCLUSION

This paper uses the conformal mapping for the complex frequency plane of a lumped element Butterworth low-pass filter, the complex frequency planes of a transmission-line low-pass filter having zeros of m'th order in the passband and poles of mth order in the stopband and of a transmission-line low-pass filter having the Butterworth characteristic in the passband and poles of mth order in the stopband are derived, and the design equations strictly fulfilling the specification are derived. The former transmission-line low-pass filter has an improved skirt attenuation performance than a Chebyshev transmission-line low-pass filter, it is positioned about in the intermediate between the Chebyshev type and the elliptic-function type, and it has more smooth delay characteristic than these two types. The latter transmission-line low-pass filter has a better skirt attenuation performance than the Butterworth low-pass filter and a better delay characteristic than the Chebyshev low-pass filter. Accordingly, the transmission-line low-pass filters treated in this paper should be considered viable alternatives to Butterworth, Chebyshev, and elliptic-function filters. The design curves given in Figs. 6 and 7 are useful for many practical applications.

APPENDIX

Equation (10) can be obtained as follows: When the negative line charge $-nQ/2$ is placed at the pole positions $j1.0$ and $-j1.0$ in the ζ-plane, the positive line charge $m'Q$ is placed at the zero point positions $j\zeta_0$ and $-j\zeta_0$, and the positive line charge $(n-2m')Q$ is placed in the zero point at the infinite point, the amount of the total charge becomes zero, and the complex potential χ_ζ in the ζ-plane becomes

$$\begin{aligned}\chi_\zeta &= -nQ/2\log(\zeta-j1.0)-nQ/2\log(\zeta+j1.0)\\ &\quad+m'Q\log(\zeta-j\zeta_0)+m'Q\log(\zeta+j\zeta_0)\\ &=-Q\log(\zeta^2+1)^{n/2}(\zeta^2+\zeta_0^2)^{-m'}. \end{aligned}\tag{39}$$

Next, the negative line charge $-pQ$ is placed in the pole position $j1.0$ and $-j1.0$ in the w-plane, the negative line charge $-(n/2-p-m)Q$ is placed at the pole positions jh_1 and $-jh_1$, the negative line charge $-mQ$ is placed at the pole positions jh_2 and $-jh_2$, the positive line charge $m'Q$ is placed at the zero point positions jw_0 and

$-jw_0$, and the positive line charge $(n-2m')Q$ is placed at the zero point in the infinite point in the w-plane, so that the amount of the total charge in the w-plane becomes zero, and then the complex potential χ_w in the w-plane is

$$\begin{aligned}\chi_w = & -pQ\log(w-j1.0)-pQ\log(w+j1.0)\\ & -(n/2-p-m)Q\log(w-jh_1)\\ & -(n/2-p-m)Q\log(w+jh_1)\\ & -mQ\log(w-jh_2)-mQ\log(w+jh_2)\\ & +m'Q\log(w-jw_0)+m'Q\log(w+jw_0)\\ = & -Q\log(w^2+1)^p(w^2+h_1^2)^{n/2-p-m}\\ & \cdot(w^2+h_2^2)^m(w^2+w_0^2)^{-m'} \qquad (40)\end{aligned}$$

where Q is the unit line charge, and $1/2\pi\epsilon$ is omitted.

Since the complex potential of the two-dimensional electrostatic field is analogous to the operating transmission function of the network [13], it is necessary that (39) and (40) become equal in order that the operating transmission function may not be allowed to change by the transformation from the ζ-plane to the w-plane. Accordingly, by equalizing (39) to (40), the (41) (that is (10)) is derived as follows:

$$(w^2+1)^p(w^2+h_1^2)^{n/2-p-m}(w^2+h_2^2)^m(w^2+w_0^2)^{-m'} = (\zeta^2+1)^{n/2}(\zeta^2+\zeta_0^2)^{-m'}. \qquad (41)$$

Equation (29) also is derived by the same method.

References

[1] R. Levy, "Filters with single transmission zeros at real or imaginary frequencies," *IEEE Trans. Microwave Theory Tech.*, vol. MTT-24, pp. 172–181, Apr. 1976.

[2] M. C. Agarwal and A. S. Sedra, "On designing sharp cut off low pass filters," *IEEE Trans. Audio Electroacoust.*, vol. AU-20, pp. 138–141, June 1972.

[3] A. Budak and P. Aronhime, "Maximally flat low pass filters with steeper slopes at cut off," *IEEE Trans. Audio Electroacoust.*, vol. AU-18, pp. 63–66, Mar. 1970.

[4] S. C. Dutta Roy, "On maximally flat sharp cut off low pass filters," *IEEE Trans. Audio Electroacoust.*, vol. AU-19 pp. 58–63, Mar. 1971.

[5] M. C. Horton and R. J. Wenzel, "General theory and design of optimum quarter wave TEM filters," *IEEE Trans. Microwave Theory Tech.*, vol. MTT-13, pp. 316–327, May 1965.

[6] ——, "Realization of microwave filters with equal ripple response in both pass and stop bands," in *Proceedings of the Symposium on Generalized Networks*. New York: Polytechnic Press, 1966.

[7] L. Fraiture and J. Neirynck, "Optimum elliptic-function filters for distributed constant systems," *IEEE Trans. Microwave Theory Tech.*, pp. 482–483, Aug. 1967.

[8] M. C. Horton and R. J. Wenzel, "The effectiveness of component elements in commensurate line length filters," *IEEE Trans. Microwave Theory Tech.*, pp. 555–557, Aug. 1968.

[9] P. I. Richards, "Resistor-transmission-line circuits," *Proc. IRE*, vol. 36, pp. 217–220, Feb. 1948.

[10] R. Sato, *Transmission Circuits* (*Denso-Kairo*). Tokyo, Japan: Korona-sha, 1963, pp. 380–400.

[11] J. Huruya and R. Sato, "A design method of low pass filters whose slope characteristic was improved," *Trans. Inst. Electron. Commun. Eng. Jap.*, vol. 60-A, pp. 645–652, July 1977.

[12] B. M. Schiffman, "A multiharmonic filter designed by an exact method," *IEEE Trans. Microwave Theory Tech.*, vol. MTT-12, pp. 512–516, Sept. 1964.

[13] S. Darlinton, "The potential analogue method of networks synthesis," *Bell Syst. Tech. J.*, vol. 30, pp. 315–365, Apr. 1951.